

🔗 Evaluation of Surface Fluxes in ERA-Interim Using Flux Tower Data

CHUNLÜE ZHOU AND KAICUN WANG

College of Global Change and Earth System Science, Beijing Normal University, and Joint Center for Global Change Studies, Beijing, China

(Manuscript received 26 July 2015, in final form 9 December 2015)

ABSTRACT

Surface air temperature T_a is largely determined by surface net radiation R_n and its partitioning into latent (LE) and sensible heat fluxes (H). Existing model evaluations by comparison of absolute flux values are of limited help because the evaluation results are a blending of inconsistent spatial scales, inaccurate model forcing data, and imperfect parameterizations. This study further evaluates the relationships of LE and H with R_n and environmental parameters, including T_a , relative humidity (RH), and wind speed (WS), using ERA-Interim data at a $0.125^\circ \times 0.125^\circ$ grid with observations at AmeriFlux sites from 1998 to 2012. The results demonstrate ERA-Interim can roughly reproduce the absolute values of environmental parameters, radiation, and turbulent fluxes. The model performs well in simulating the correlation of LE and H with R_n , except for the notable correlation overestimation of H against R_n over high-density vegetation (e.g., deciduous broadleaf forest, grassland, and cropland). The sensitivity of LE to R_n in the model is similar to that observed, but that of H to R_n is overestimated by 24.2%. Over the high-density vegetation, the correlation coefficient between H and T_a is overestimated by over 0.2, whereas that between H and WS is underestimated by over 0.43. The sensitivity of H to T_a is overestimated by $0.72 \text{ W m}^{-2} \text{ }^\circ\text{C}^{-1}$, whereas that of H to WS in the model is underestimated by $16.15 \text{ W m}^{-2} (\text{m s}^{-1})^{-1}$ over all of the sites. The model cannot accurately capture the responses of evaporative fraction [EF; $\text{EF} = \text{LE} / (\text{LE} + H)$] to R_n and environmental parameters. This calls for major research efforts to improve the intrinsic parameterizations of turbulent fluxes, particularly over high-density vegetation.

1. Introduction

Land surface is heated by solar shortwave radiation and emits longwave radiation to cool itself. The surface net radiation R_n , which is the sum of net solar shortwave radiation R_{sn} and the net longwave radiation R_{ln} , can be partitioned into the latent heat flux (LE), sensible heat flux (H), and ground heat flux (G). The flux H directly heats the atmosphere through various sizes of turbulences, and LE transports water from the land surface to the atmosphere, absorbing energy through phase changes of water from liquid (or ice) to gas and leaving some remaining energy for H (Wang and Dickinson 2012). The partitioning of R_n between LE and H depends on surface attributes [e.g., vegetation growth and soil moisture (SM)] and atmosphere conditions (e.g.,

vapor pressure deficit and surface air temperature) (IPCC 2013), which has a significant impact on climate change, particularly the response of land surface air temperature and the water cycle, and vice versa (Andrews et al. 2009; Stephens et al. 2012). Under a changing climate, surface characteristics and atmospheric conditions have been evolving (IPCC 2013), and surface incident solar radiance (or R_n) has been changing (Wang and Dickinson 2013), which are inevitably influencing the partitioning of R_n between LE and H associated with climate forcings and climate change processes (Wang 2010, Wang et al. 2010).

Thus, it is critical to evaluate the performance of global climate models in simulating R_n and its partitioning into LE and H . Existing studies focused on comparing the absolute values of these turbulent fluxes with observations (including the in situ and remote sensing observations) (Bourras 2006; Jiménez et al. 2011; Kubota et al. 2003; Szczypta et al. 2011; Yao et al. 2014). Moreover, between-model comparisons are used to improve the land model schemes. For example, sixteen land surface schemes from the Project for the Intercomparison of Land-Surface Parameterization

🔗 Denotes Open Access content.

Corresponding author address: Kaicun Wang, College of Global Change and Earth System Science, Beijing Normal University, No. 19 Xijiekouwai St., Beijing 100875, China.
E-mail: kcwang@bnu.edu.cn

DOI: 10.1175/JCLI-D-15-0523.1

Schemes (PILPS) with the same forcing data were compared to diagnose model shortcomings for improvements (Henderson-Sellers et al. 1993; Pitman et al. 1999; Wood et al. 1998). Evaluation of the biosphere-atmosphere schemes, including BATS, BATS2, SiB, and SiB2, indicated that the excessive sensitivity of the stomatal response to the atmospheric humidity deficit should be developed, and the root distribution depth should be specified in the models (Sen et al. 2000). The Community Land Model (CLM) was examined by the response of land-atmosphere exchanges to climatic forcings, and the deficiencies in hydrological and biophysical parameterizations have been detected and improved to largely decrease the LE and H errors (Stöckli et al. 2008).

However, the discrepancies between the simulated and observed LE and H values may arise from many sources, such as the inconsistent scales of simulation and observations, inaccurate forcing data of the model simulations, and imperfect parameterizations of H and LE fluxes (Brutsaert 1999; Chen and Zhang 2009; Maurer et al. 2002; Pitman and Henderson-Sellers 1998; Santanello et al. 2009; Wang and Dickinson 2012). The direct comparison of absolute values complicates the model evaluation and makes the evaluation results less useful in improving model simulations.

To address these issues, a new method, which considers the correlation coefficient and sensitivity of LE and H to R_n and other environmental parameters [i.e., air temperature T_a , relative humidity (RH), and wind speed (WS)], is proposed here to evaluate the partitioning between LE and H from the European Centre for Medium-Range Weather Forecasts (ECMWF) interim reanalysis (ERA-Interim). A quantitative evaluation of these relationships can provide insight into the intrinsic model capability of partitioning the available energy into LE and H . Therefore, such a study about land-atmosphere processes is expected to provide some constructive information to improve the simulation and predictive skills of climate sensitivity in models.

Here, ERA-Interim is selected because it has relatively accurate land forcing data, including in situ and remote sensing observations, and physical coherence (Dee et al. 2011). Its latest version for land surface fluxes also has a very high spatial resolution of $0.125^\circ \times 0.125^\circ$. We find that although the absolute values of the turbulent fluxes can be well captured by the model, the ERA-Interim land model cannot accurately describe the responses of H and evaporative fraction (EF) to R_n and some environmental parameters in high-density vegetation regions, particularly for deciduous broadleaf forest (DBF), grassland

(GRA), and cropland (CRO). Therefore, this issue requires major research efforts to improve the parameterizations of the ERA-Interim land model over these land-cover types.

2. Dataset description

a. ERA-Interim dataset

ERA-Interim is produced with the observation fields, the forecast model, and a four-dimensional variational assimilation system (4D-VAR), which assimilates a great many of the basic upper-air atmospheric fields (such as satellite radiances, temperature, wind vectors, specific humidity, and ozone), and then uses the forecast model to constrain the atmospheric analysis in 12-hourly analysis cycles. While producing a forecast, the model estimates a wide variety of physical parameters such as precipitation, turbulent fluxes, radiation fields, cloud properties, soil moisture, and so on, which are not constrained by their own direct measurements. Furthermore, ERA-Interim conducts a completely automated bias correction for satellite radiance observations and surface pressure after a suite of quality control and blacklist data selection. After the upper-air atmospheric 4D-VAR analysis, the model state in ERA-Interim is adjusted by loop for systematic errors with an optimal interpolation scheme of near-surface observations from weather stations such as T_a , RH, 10-m wind vectors, surface pressure, and so forth (Trémolet 2004; Veerse and Thepaut 1998), and the Cressman-type interpolation is used to analyze the station observations of snow depth and satellite-retrieved snow cover (Dee et al. 2011).

Its high-resolution forecast and data assimilation system adopts the T1279 spectral model based on a spherical harmonics expansion (i.e., T1279 to identify truncation at wavenumber 1279) and has the horizontal resolution of N640 in a reduced Gaussian grid ($\sim 0.141^\circ \times 0.141^\circ$ in a geographic latitude-longitude grid, approximately $15 \times 15 \text{ km}^2$). Finally, outputs of ERA-Interim are bilinearly interpolated to ten various resolutions from 0.125° to 3° , including 0.75° , 1° , and 2.5° .

This study investigates the partitioning of R_n and its relationship to the environment using ERA-Interim data with AmeriFlux observations. To make good use of the data at the AmeriFlux site along the coastal line (Fig. 1) and substantially reduce the noise effect in comparison between tower sites and model grid cells, the resolution of $0.125^\circ \times 0.125^\circ$ is selected to avoid the properties of the ocean, other than the $\sim 0.7^\circ \times 0.7^\circ$

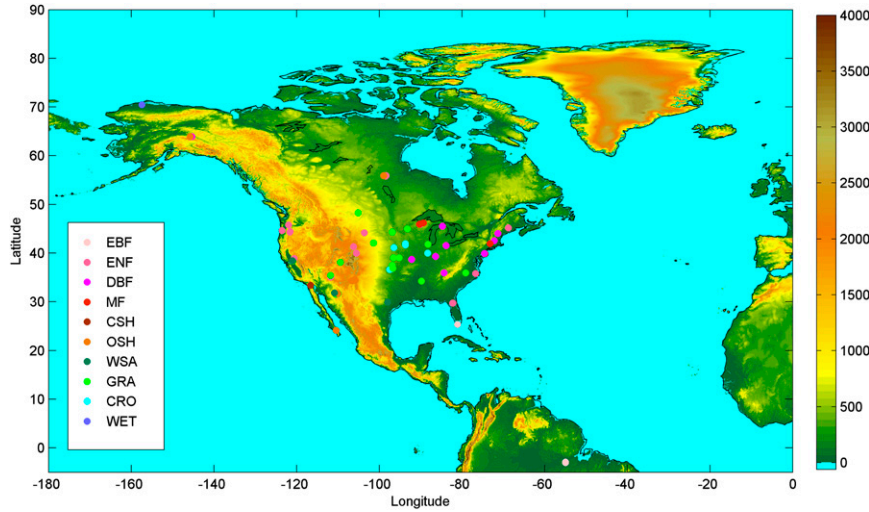


FIG. 1. The 84 sites from the AmeriFlux network are shown on the elevation map (unit: m) of the global 30-arc-s elevation dataset (GTOPO30). The sites are distributed over a range of land-cover types: EBF, evergreen needleleaf forest (ENF), DBF, mixed forest (MF), CSH, open shrubland (OSH), WSA, GRA, CRO, and wetland (WET). More site information is available online (<http://ameriflux.lbl.gov/>). GTOPO30 was developed over a 3-yr period (ending in late 1996) through a collaborative effort led by the U.S. Geological Survey's Center for Earth Resources Observation and Science (EROS).

ERA-Interim data. Energy (including R_{sn} , R_{ln} , LE, and H) and environmental parameters (including T_a , RH, and WS) from ERA-Interim synoptic monthly averages of forecast accumulations of 12 h ahead from 0000 and 1200 UTC at the grid resolution of $0.125^\circ \times 0.125^\circ$ were downloaded from the ECMWF website (<http://apps.ecmwf.int/datasets>). The term R_n in ERA-Interim is the sum of R_{sn} and R_{ln} . The term R_{sn} (R_{ln}) is the total of surface downward and upward shortwave (long-wave) radiation. The surface air and dewpoint temperature height is 2 m, and the wind speed height is 10 m. Soil moisture (level 1) is expressed as the volumetric water content ($\text{m}^3 \text{m}^{-3}$; unit: %) above the top 7 cm.

According to the seventeen International Geosphere-Biosphere Programme (IGBP) land-cover types, the land-cover types in ERA-Interim are derived from Advanced Very High Resolution Radiometer (AVHRR) data at 1-km resolution and ancillary information and are kept fixed in time (Dee et al. 2011; Loveland et al. 2000). Based on the tiled ECMWF scheme for surface exchanges over land (TESSEL) in the ERA-Interim model (Dee et al. 2011; Viterbo and Beljaars 1995; Viterbo et al. 1999), in which each grid box is divided into fractions with up to six fractions over land (i.e., bare ground, low and high vegetation, intercepted water, and shaded and exposed snow) and up to two fractions over sea and freshwater bodies (open and frozen water), the turbulent fluxes (including LE and H) are calculated by a resistance

parameterization with the Monin-Obukhov formulation over different fractions:

$$H_i = \rho_a c_p |U_L| C_{H,i} (T_L + g z_L - T_{sk,i}), \quad (1)$$

$$\text{LE}_i = \rho_a |U_L| C_{H,i} [q_L - q_{\text{sat}}(T_{sk,i})], \quad \text{and} \quad (2)$$

$$\text{LE}_i = \frac{\rho_a}{r_a + r_c} [q_L - q_{\text{sat}}(T_{sk,i})], \quad (3)$$

where i represents the fraction; H_i is sensible heat flux in the i^{th} fraction; LE_i is latent heat flux in the i^{th} fraction; ρ_a is the air density; c_p is the heat capacity of moist air; g is the acceleration of gravity; and $|U_L|$, T_L , q_L , and z_L are the wind speed, temperature, humidity, and height of the lowest atmospheric model level, respectively. The term q_{sat} is saturated specific humidity. The term $T_{sk,i}$ is the skin temperature for the i^{th} fraction. The term $C_{H,i}$ is the turbulent exchange coefficient, which varies from fraction to fraction because of different atmospheric stabilities; $r_a = (|U_L| C_{H,i})^{-1}$, and r_c is a function of downward shortwave radiation, leaf area index (LAI), average unfrozen root soil water, atmospheric water vapor deficit, and a minimum stomatal resistance.

Specifically, for snow on low vegetation, the turbulent fluxes of heat and water vapor are given by Eqs. (1) and (2), whereas for a vegetation-covered surface, an additional canopy resistance r_c is added to calculate LE according to Eq. (3). Therefore, the total turbulent fluxes in a grid box are expressed as an area-weighted average

of all fractions. To modulate the partitioning of energy and water fluxes, the maximum value of soil water content in any layer corresponds to saturation ($0.472 \text{ m}^3 \text{ m}^{-3}$) and only occurs during short periods with water loss through bottom drainage in the TESSEL scheme. Additionally, the vegetation seasonality is described by the LAI (Dee et al. 2011).

b. AmeriFlux dataset

AmeriFlux data over 84 stations are used to assess the performance of the ERA-Interim model (Fig. 1), which are not assimilated by the ERA-Interim. The AmeriFlux sites were originally designed to measure the carbon, water, and heat fluxes (including LE and H) around the adjacently identical land-cover types. The AmeriFlux network measures T_a , RH, WS, SM, R_n , R_{sn} , and R_{in} over approximately 140 stations across a range of land-cover types (Baldocchi et al. 2001). These data are publicly available online (<http://AmeriFlux.ornl.gov/>). The turbulent fluxes are measured by eddy-covariance (EC) systems. SM (in volumetric percentage unit) is measured by time domain reflectometry (TDR). TDR measures the transit time of waves along a probe in the soil based on the properties of electromagnetic waves.

All data except for SM are measured above the canopy, and the flux tower height at study sites varies from 1.5 to 60 m above the ground surface. The land-cover types include deciduous and evergreen forest, closed shrubland (CSH), grassland, cropland, and woody savanna (WSA) (Fig. 1), based on the 17 IGBP land-cover types from Moderate Resolution Imaging Spectroradiometer (MODIS) sensors. The climate type varies from arid to humid, and the climate varies from tropical and temperate to Mediterranean.

Although the EC method is considered to be the best method for measuring the H and LE fluxes, it suffers from an unclosed energy problem (Twine et al. 2000; Wilson et al. 2002). To reduce the impact of energy imbalance on the evaluation results, the AmeriFlux sites at which the residual from R_n minus LE and H is less than $1/5$ of R_n are selected for the unavailability of the ground heat flux at most sites. Furthermore, the relationship between the evaporative fraction [EF = LE/(LE + H)] and R_n (and the environmental parameters) was evaluated. The EF value obtained by the EC method is believed to be more reliable than LE or H (Twine et al. 2000; Wilson et al. 2002).

The AmeriFlux data are available at a 30- or 60-min temporal resolution. To reduce the impact of missing data on monthly averages, monthly data averaged from monthly diurnal data (monthly mean half-hourly or hourly data of R_n , LE, H , T_a , RH, and WS) are calculated and used in this study. To maintain as

comprehensive a site-specific characteristic as possible (e.g., multiseasonal signals), it requires the data length of a site to be no less than 24 months, which is sufficient enough to perform a statistical analysis with degrees of freedom. After consideration of the energy balance ratio and data length, the 84 AmeriFlux sites with a time span from 1998 to 2012 are selected in this study.

To assess the performance of the ERA-Interim model, the sensitivity s of LE, H , and EF to R_n and the environmental factors, including T_a , RH, and WS, is calculated based on Eq. (4):

$$y = sx + b + \varepsilon, \quad (4)$$

where, y is monthly LE, H , and EF; and x is monthly R_n , T_a , RH, and WS, respectively. The s is the corresponding sensitivity, b is the interpolate when $x = 0$, and ε is the error of equation.

This sensitivity of LE (H , EF) helps depict the magnitude in the response to climatic change. Pearson's correlation and a two-tailed t test are applied to calculate their correlation coefficients.

3. Results

a. Absolute value evaluation

The monthly R_n , R_{sn} , and R_{in} correspond well with the observed values, with a correlation coefficient r up to 0.9 and a relative error of approximately 25% or less (Figs. 2a–c). The ERA-Interim land model performs well in simulating the absolute values of LE and H , with an r greater than 0.82, whereas the bias of the simulated H , 3.23 W m^{-2} (relative bias of 30.12%), is better than that of LE, 12.91 W m^{-2} (relative bias of -8.6%) (Figs. 2d,e).

The environmental parameters simulated by the ERA-Interim land model are validated by in situ and remote sensing observations at different spatiotemporal scales (Albergel et al. 2015; Balsamo et al. 2015; Bao and Zhang 2013; Boisvert et al. 2015; Mooney et al. 2011; Su et al. 2013; Szczypka et al. 2011; Wang and Zeng 2012). Figure 2f shows that T_a in the model is consistent with that from AmeriFlux [$r = 0.99$; bias = 0.05°C ; standard deviation (STD) = 1.74°C]. Figure 2g shows that RH in the model corresponds well with the observed RH, with an r of 0.85, a bias of -0.42% , and an STD of 8.15% (relative STD of 12.21%). Figure 2h illustrates that WS in the model correlates against the observations, with an r of 0.56, a bias of 0.74 m s^{-1} , and an STD of 0.96 m s^{-1} (relative STD of 35.40%). Additionally, the low correlation of SM between the model and observations ($r = 0.32$; Fig. 2i) at AmeriFlux sites is likely associated with the SM constraint of 47.2% in the model, vegetation

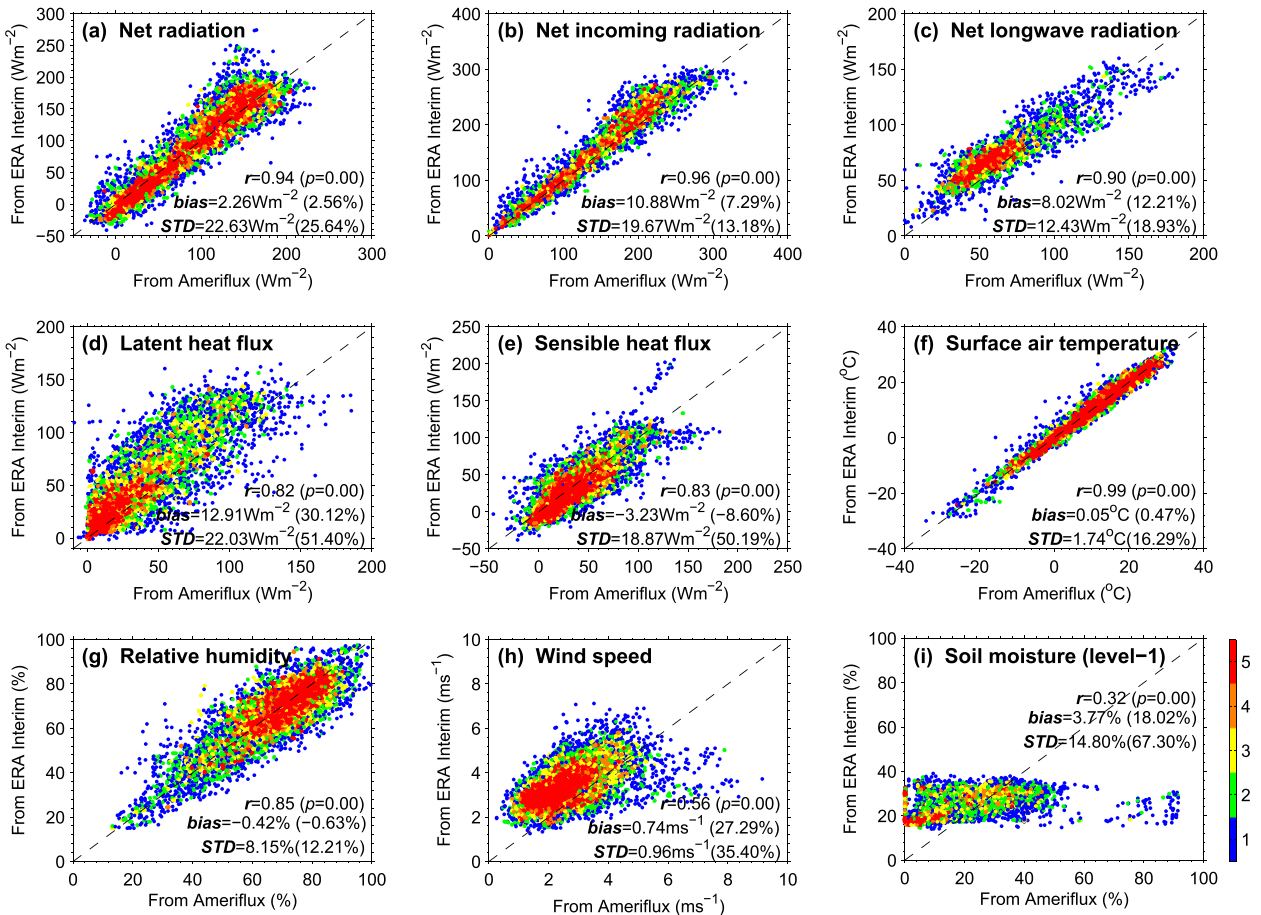


FIG. 2. Comparisons of (a) net radiance, (b) net shortwave radiance, (c) net longwave radiance, (d) LE, (e) H , (f) surface air temperature, (g) RH, (h) WS, and (i) SM at level 1 from ERA-Interim and AmeriFlux are shown as the density scatterplot. The color bar expresses the scatter density, which is defined as the number of data dots in 100×100 axis grids. Toward red indicates a dense distribution and toward blue indicates a sparse distribution. Net radiation is calculated as R_{sn} minus R_{in} from the ERA-Interim data. The statistical scores, including the correlation coefficient r , bias, and STD, are calculated for every variable.

root distribution and its surrounding moisture (Albergel et al. 2012). SM in ERA-Interim is notably overestimated particularly for dry land (Fig. 2i), which is consistent with the evaluation of SM from the previous work (Albergel et al. 2012), but is notably underestimated over some humid regions.

b. Responses of LE and H to surface net radiation

The relative magnitude of partitioning of R_n into LE and H has an important role in climate change. Here, this partitioning of R_n from the ERA-Interim land model is evaluated. Figure 3a shows that the correlation between LE and R_n in the model is comparable to that observed by AmeriFlux over all of the sites. Figure 4a demonstrates that the correlation between H and R_n in the model has an average of 0.89 over all land-cover types, which is significantly higher than the observed 0.68 from AmeriFlux. In ERA-Interim, the correlation

of H against WS cannot be reproduced by the model (Figs. 4c,g). This indicates that the parameterization of H in the ERA-Interim model is too oversimplified to accurately reproduce the complex dependences and feedbacks of H on environmental parameters (i.e., WS; more details in the following section). This issue is more important for the high-density vegetation regions. The overestimation of correlation coefficient between H and R_n is more than 0.25 (averaged relative error of 69%) over highly dense vegetation areas, including DBF, CRO, and GRA (Fig. 4a).

The site-averaged sensitivity of LE to R_n (0.44) in the model is comparable to the observed sensitivity (0.43) (Fig. 3b), whereas that of H to R_n (0.33) from AmeriFlux is overestimated by the model (0.41; relative error of 24.2%) over all land-cover types (Fig. 4b). The reason for this sensitivity overestimation is the same as that for their correlation overestimation. This intensifies the

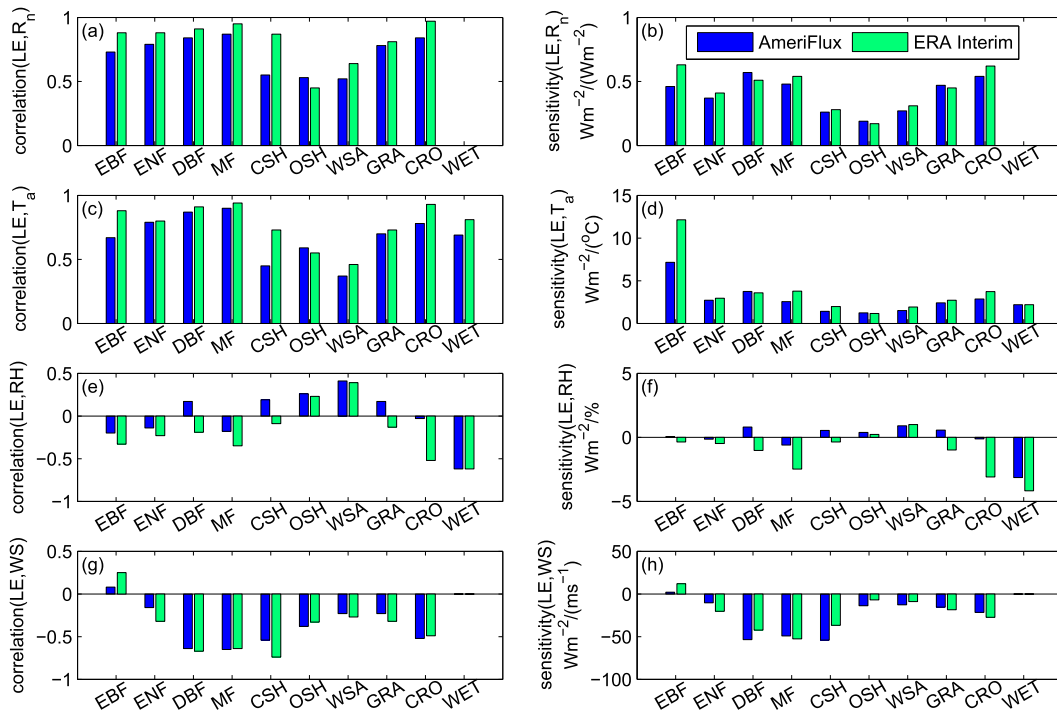


FIG. 3. (left) The average correlation and (right) sensitivity of LE with (a),(b) R_n , (c),(d) T_a , (e),(f) RH, and (g),(h) WS over different land-cover types, including EBF, ENF, DBF, MF, CSH, OSH, WSA, GRA, CRO, and WET. The blue bar is based on the AmeriFlux observations, and the green bar is based on ERA-Interim data.

response of H to an increase in R_n in the ERA-Interim model, which has a substantial effect on the simulation of energy partitioning and climate change. Monthly data are used to calculate the sensitivity and the sum of the sensitivities of LE/R_n and H/R_n in the model, producing a value of 0.85, which is considerably less than unity because of the significant seasonal cycle of G (Hsieh et al. 2009; Kustas et al. 2000; Ogée et al. 2001).

To obtain the energy closure ratio, it is necessary to calculate the multiyear averaged values of LE , H , and R_n and then calculate the LE/R_n and H/R_n ratios in the ERA-Interim model and AmeriFlux observations. The values of LE/R_n and H/R_n are 0.53 and 0.42 in the ERA-Interim model, respectively, and are 0.47 and 0.43 in the AmeriFlux observations, respectively. These results are consistent with the over- and underestimated evaluation results using absolute values of LE and H (see section 3a). The correlation and sensitivity analyses made in this section and the following section permit us to examine the responses of LE and H to R_n and other environmental parameters, which are indicators of how land-atmosphere interactions change with climate and environmental changes.

c. Responses of LE and H to environmental parameters

To evaluate how R_n is partitioned into LE and H , the correlation and sensitivity of LE and H to environment

parameters, including T_a , RH, and WS, over different land-cover types, are investigated in this section.

Figure 4c illustrates a similar correlation between H against T_a to that of H against R_n as shown in Fig. 4a. Similarly, the model significantly overestimates the correlation between H and T_a by more than 0.2 over high-density vegetation (DBF, CRO, and GRA) (Fig. 4a) and performs well over other land-cover types with respect to the AmeriFlux observations (Fig. 4a). These overestimations imply that the model may omit some important factors influencing H . The correlation of H to WS in the model is underestimated by more than 0.43 and even shows the opposite sign as the observations over DBF, CSH, GRA, and CRO (Fig. 4g). An increase in WS may induce a low aerodynamic resistance r_a over high-density vegetation based on Eq. (3), accumulating large LE and leaving little energy to H , resulting in an underestimation of H against WS in the model. Moreover, r_c is only simply parameterized based on different vegetation types (Dee et al. 2011). These factors could explain why the correlation of H and R_n over high-density vegetation was overestimated.

The sensitivity of H to T_a in the model is consistently overestimated by $0.72 \text{ W m}^{-2} \text{ } ^\circ\text{C}^{-1}$ over all of the sites (Fig. 4d). This overestimated sensitivity may be due to the insufficient estimation of the soil water availability and the unrealistic root depth in the model (Wang and

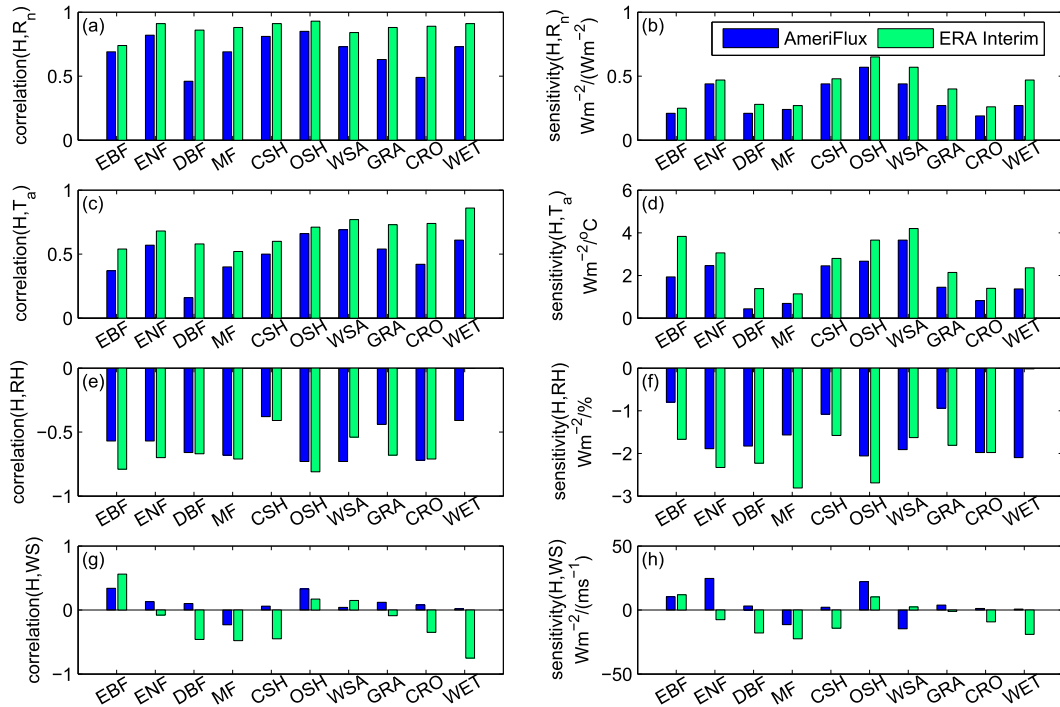


FIG. 4. (left) The average correlation and (right) sensitivity of H with (a),(b) R_n , (c),(d) T_a , (e),(f) RH, and (g),(h) WS over different land-cover types, including EBF, ENF, DBF, MF, CSH, OSH, WSA, GRA, CRO, and WET. The blue bar is based on AmeriFlux observations, and the green bar is based on ERA-Interim data.

Dickinson 2012). Moreover, the sensitivity of H to WS in the model is notably underestimated by $16.15 \text{ W m}^{-2} (\text{m s}^{-1})^{-1}$ over all of the sites (Fig. 4h). The large discrepancies in these sensitivities indicate the inaccuracy of the response of H to such environmental parameters as T_a and WS in the ERA-Interim land model, particularly over high-density vegetation. Therefore, the parameterization deficiency in simulating the impact of T_a and WS on H results in the overestimated response of H to R_n in the model, particularly over high-density vegetation.

Moreover, the site-averaged correlation of H against RH in the model (-0.59) is similar to that of AmeriFlux (-0.60) (Fig. 4e), and their site-averaged sensitivity in the model ($-1.88 \text{ W m}^{-2} \%^{-1}$) is comparable to that observed from AmeriFlux ($-1.62 \text{ W m}^{-2} \%^{-1}$) over all land-cover types (Fig. 4f).

Figure 3c demonstrates that LE is positively correlated with T_a (average r of 0.68 from AmeriFlux and 0.77 from ERA-Interim), which is similar to the result in the controlled experiment from PILPS (Qu et al. 1998). The correlation between LE and T_a can be well simulated by the ERA-Interim model. The sensitivity of LE to T_a in the model corresponds well with the AmeriFlux observations (Fig. 3d). The good agreement of the sensitivity of LE to T_a between model and observation shows that

the different spatial scales from model and observation do not significantly impact the sensitivity, but the scales do impact the absolute value of LE (Fig. 1d). Figure 3g indicates that the averaged correlation of LE against WS (-0.39) in the model is similar to that from AmeriFlux (-0.37) over all land-cover types. Accordingly, the average sensitivities of LE to WS are $-22.41 \text{ W m}^{-2} (\text{m s}^{-1})^{-1}$ in the model and $-25.40 \text{ W m}^{-2} (\text{m s}^{-1})^{-1}$ in the AmeriFlux observations (Fig. 3h). Furthermore, the response of LE to variance in WS in the model is consistent with the observations for each land-cover type (Figs. 3g,h). Therefore, the model can capture the response of LE to the environmental parameters.

d. Responses of EF to net radiation and environmental parameters

During the land-atmosphere interaction, the partitioning of R_n into LE and H is dynamically interactive, balancing the climate system. Thus, the response of LE to R_n and other environmental conditions may influence the response of H and vice versa. To strictly avoid energy imbalance, when considering LE and H simultaneously, the responses of EF [EF = LE/($R_n - G$) = LE/(LE + H)] to R_n and other environmental parameters—including T_a , RH, and WS—are evaluated below to better describe the land-atmosphere interaction,

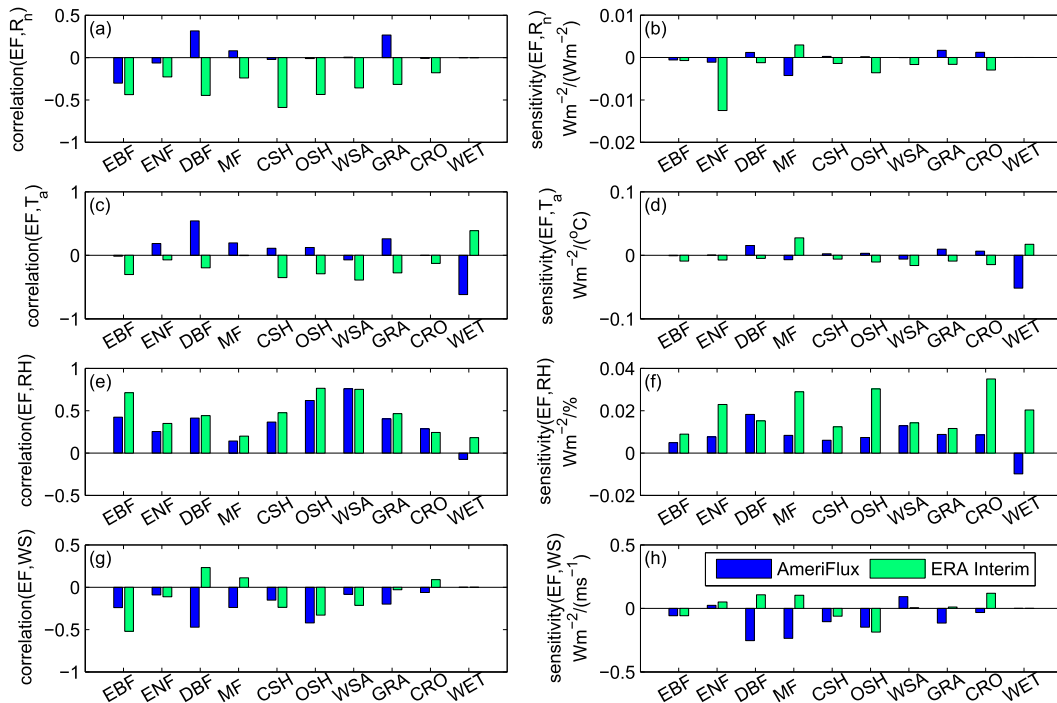


FIG. 5. (left) The average correlation and (right) sensitivity of EF with (a),(b) R_n , (c),(d) T_a , (e),(f) RH, and (g),(h) WS over different land-cover types, including EBF, ENF, DBF, MF, CSH, OSH, WSA, GRA, CRO, and WET. The blue bar is based on AmeriFlux observations, and the green bar is based on ERA-Interim data.

including their responses and feedbacks under climate change conditions.

Figure 5a shows that EF is irrelevant to R_n in the AmeriFlux observations, whereas the correlation between EF and R_n is significantly negative in the model, with an average r of -0.36 over all of the sites. This correlation may incorrectly result from simple parameterizations of r_c and turbulent exchange coefficient, just based on land-cover types. Accordingly, the sensitivity of EF to R_n in the model is negatively correlated with the observations, with an r of -0.48 (Fig. 5b). This opposite sensitivity in the ERA-Interim model will erroneously depict the partitioning of surface available energy between LE and H , which is of great importance for the response of the hydrological cycle and temperature change. Figure 5c illustrates that EF is positively correlated with T_a in the AmeriFlux observations but negatively correlated with T_a in the model over most land-cover types. Although the correlation between EF and RH can be simulated by the model (Fig. 5e), the model overestimates the sensitivity of EF to RH, with a relative error of 175% (Fig. 5f). The averaged sensitivity of EF to RH over all land-cover types is 0.0073 ($\%^{-1}$) from AmeriFlux and 0.0200 ($\%^{-1}$) in the model.

By validating the correlation and sensitivity of LE (H and EF) to R_n and other environmental parameters,

including T_a , RH, WS, and different land-cover types, in the ERA-Interim model using AmeriFlux observations, the results above provide a constructive guidance for simulating the partitioning of R_n into LE and H (EF) in the ERA-Interim model, a state-of-the-art global climate model. For example, improvements are required for aerodynamic and canopy resistances, vegetation root depth, and the turbulent exchange coefficient over high-density vegetation.

4. Conclusions and discussion

The response and feedback of LE and H to R_n and other environmental conditions, including T_a , RH, WS, and different land-cover types, play important roles in climate change and climate sensitivity. Given an increase in the available energy, the relative magnitudes of partitioning into LE and H have a vital impact on the hydrological cycle and temperature change. This study provides a new method to evaluate the performance of the ERA-Interim model in partitioning R_n into LE and H . The correlation and sensitivity analyses of LE and H indicate that the partitioning is closely correlated with land-cover type.

Overall, the model can well capture the response of LE to R_n . Additionally, the correlation and sensitivity of

LE to environmental parameters, including T_a , RH, and WS, are similar to the observed values. This result is different from the overestimated sensitivity of LE from regional climate models (Winter and Eltahir 2010). Second, the model clearly overestimates the correlation between H and R_n over high-density vegetation (DBF, GRA, and CRO). Compared with AmeriFlux, the sensitivity of H to R_n is overestimated by 24.2% at all of the sites. There are two reasons for the overestimations in correlation and sensitivity of H to R_n in the model. First, the correlation between H and T_a is overestimated by more than 0.2, and that between H and WS in the model is underestimated by more than 0.43 over high-density vegetation (DBF, CRO, and GRA). Second, the sensitivity of H to T_a is largely overestimated by $0.72 \text{ W m}^{-2} \text{ } ^\circ\text{C}^{-1}$, and the sensitivity of H to WS in the model is notably underestimated by $16.15 \text{ W m}^{-2} (\text{m s}^{-1})^{-1}$ over all of the sites. Therefore, the overestimated response of H is closely correlated with the insufficient estimation of soil water availability, the unrealistically vegetation root distribution, and aerodynamic resistance and canopy resistance parameterization.

The discrepancies between the model results and observations in reproducing the relationship between H (and LE) and R_n or the environmental factors accumulate in the relationship between the evaporative fraction [$\text{EF} = \text{LE}/(\text{LE} + H)$] and R_n or the environmental factors. The relationship between EF and R_n or environmental factors cannot be well simulated by the model with respect to the AmeriFlux observations. The sign of the correlation between EF and T_a in the model is the opposite of that obtained from the observations. The sensitivity of EF to RH is overestimated by 175%.

Therefore, the response of LE and H to the available energy and environmental conditions over high-density vegetation should be improved considerably. This requires further detection of the factors controlling H and LE at different time scales as well as further efforts in improving the aerodynamic resistance and canopy resistance over high-density vegetation. Furthermore, the simulation of SM in the model should be improved, which has a significant impact on the partitioning of the available energy into LE and H . Therefore, these results offer significant guidance to further improve the ERA-Interim model.

In summary, despite the good performance of the absolute value of the turbulent fluxes in the model, this direct comparison provides limited insight into model performance, which should be cautiously regarded as a method of model evaluation under changing climates for mixing many potential sources of error, including sampling error, instrument bias, and uncertainty in the flux computational algorithms. In this study, the results from

the sensitivity experiments of the turbulent fluxes reveal important insights into the model sensitivity and parameterization of LE and H . Furthermore, this sensitivity analysis can be a useful approach to compare model performances with different climatology and sensitivity.

Acknowledgments. This study was funded by and the National Natural Science Foundation of China (41525018 and 91337111) and the National Basic Research Program of China (2012CB955302). Considerable gratitude is given to the AmeriFlux community for making the data publicly available (<http://ameriflux.lbl.gov/>), as well as to the principal investigators and collaborators at each site. ERA-Interim data were downloaded from <http://apps.ecmwf.int/datasets>.

REFERENCES

- Albergel, C., P. de Rosnay, G. Balsamo, L. Isaksen, and J. Muñoz-Sabater, 2012: Soil moisture analyses at ECMWF: Evaluation using global ground-based in situ observations. *J. Hydrometeorol.*, **13**, 1442–1460, doi:10.1175/JHM-D-11-0107.1.
- , and Coauthors, 2015: Soil temperature at ECMWF: An assessment using ground-based observations. *J. Geophys. Res.*, **120**, 1361–1373, doi:10.1002/2014JD022505.
- Andrews, T., P. M. Forster, and J. M. Gregory, 2009: A surface energy perspective on climate change. *J. Climate*, **22**, 2557–2570, doi:10.1175/2008JCLI2759.1.
- Baldocchi, D., and Coauthors, 2001: FLUXNET: A new tool to study the temporal and spatial variability of ecosystem-scale carbon dioxide, water vapor, and energy flux densities. *Bull. Amer. Meteor. Soc.*, **82**, 2415–2434, doi:10.1175/1520-0477(2001)082<2415:FANTTS>2.3.CO;2.
- Balsamo, G., and Coauthors, 2015: ERA-Interim/land: A global land surface reanalysis data set. *Hydrol. Earth Syst. Sci.*, **19**, 389–407, doi:10.5194/hess-19-389-2015.
- Bao, X., and F. Zhang, 2013: Evaluation of NCEP–CFSR, NCEP–NCAR, ERA-Interim, and ERA-40 reanalysis datasets against independent sounding observations over the Tibetan Plateau. *J. Climate*, **26**, 206–214, doi:10.1175/JCLI-D-12-00056.1.
- Boisvert, L. N., D. L. Wu, T. Vihma, and J. Susskind, 2015: Verification of air/surface humidity differences from AIRS and ERA-Interim in support of turbulent flux estimation in the Arctic. *J. Geophys. Res.*, **120**, 945–963, doi:10.1002/2014JD021666.
- Bourras, D., 2006: Comparison of five satellite-derived latent heat flux products to moored buoy data. *J. Climate*, **19**, 6291–6313, doi:10.1175/JCLI3977.1.
- Brutsaert, W., 1999: Aspects of bulk atmospheric boundary layer similarity under free-convective conditions. *Rev. Geophys.*, **37**, 439–451, doi:10.1029/1999RG900013.
- Chen, F., and Y. Zhang, 2009: On the coupling strength between the land surface and the atmosphere: From viewpoint of surface exchange coefficients. *Geophys. Res. Lett.*, **36**, L10404, doi:10.1029/2009GL037980.
- Dee, D. P., and Coauthors, 2011: The ERA-Interim reanalysis: Configuration and performance of the data assimilation system. *Quart. J. Roy. Meteor. Soc.*, **137**, 553–597, doi:10.1002/qj.828.

- Henderson-Sellers, A., Z. L. Yang, and R. E. Dickinson, 1993: The Project for Intercomparison of Land-Surface Parameterization Schemes. *Bull. Amer. Meteor. Soc.*, **74**, 1335–1349, doi:[10.1175/1520-0477\(1993\)074<1335:TPFIOL>2.0.CO;2](https://doi.org/10.1175/1520-0477(1993)074<1335:TPFIOL>2.0.CO;2).
- Hsieh, C.-I., C.-W. Huang, and G. Kiely, 2009: Long-term estimation of soil heat flux by single layer soil temperature. *Int. J. Biometeor.*, **53**, 113–123, doi:[10.1007/s00484-008-0198-8](https://doi.org/10.1007/s00484-008-0198-8).
- IPCC, 2013: *Climate Change 2013: The Physical Science Basis*. Cambridge University Press, 1535 pp., doi:[10.1017/CBO9781107415324](https://doi.org/10.1017/CBO9781107415324).
- Jiménez, C., and Coauthors, 2011: Global intercomparison of 12 land surface heat flux estimates. *J. Geophys. Res.*, **116**, D02102, doi:[10.1029/2010JD014545](https://doi.org/10.1029/2010JD014545).
- Kubota, M., A. Kano, H. Muramatsu, and H. Tomita, 2003: Intercomparison of various surface latent heat flux fields. *J. Climate*, **16**, 670–678, doi:[10.1175/1520-0442\(2003\)016<0670:IOVSLH>2.0.CO;2](https://doi.org/10.1175/1520-0442(2003)016<0670:IOVSLH>2.0.CO;2).
- Kustas, W. P., J. H. Prueger, J. L. Hatfield, K. Ramalingam, and L. E. Hips, 2000: Variability in soil heat flux from a mesquite dune site. *Agric. For. Meteorol.*, **103**, 249–264, doi:[10.1016/S0168-1923\(00\)00131-3](https://doi.org/10.1016/S0168-1923(00)00131-3).
- Loveland, T. R., B. C. Reed, J. F. Brown, D. O. Ohlen, Z. Zhu, L. Yang, and J. W. Merchant, 2000: Development of a global land cover characteristics database and IGBP DISCover from 1 km AVHRR data. *Int. J. Remote Sens.*, **21**, 1303–1330, doi:[10.1080/014311600210191](https://doi.org/10.1080/014311600210191).
- Maurer, E. P., A. W. Wood, J. C. Adam, D. P. Lettenmaier, and B. Nijssen, 2002: A long-term hydrologically based dataset of land surface fluxes and states for the conterminous United States. *J. Climate*, **15**, 3237–3251, doi:[10.1175/1520-0442\(2002\)015<3237:ALTHBD>2.0.CO;2](https://doi.org/10.1175/1520-0442(2002)015<3237:ALTHBD>2.0.CO;2).
- Mooney, P. A., F. J. Mulligan, and R. Fealy, 2011: Comparison of ERA-40, ERA-Interim and NCEP/NCAR reanalysis data with observed surface air temperatures over Ireland. *Int. J. Climatol.*, **31**, 545–557, doi:[10.1002/joc.2098](https://doi.org/10.1002/joc.2098).
- Ogée, J., E. Lamaud, Y. Brunet, P. Berbigier, and J. M. Bonnefond, 2001: A long-term study of soil heat flux under a forest canopy. *Agric. For. Meteorol.*, **106**, 173–186, doi:[10.1016/S0168-1923\(00\)00214-8](https://doi.org/10.1016/S0168-1923(00)00214-8).
- Pitman, A. J., and A. Henderson-Sellers, 1998: Recent progress and results from the project for the intercomparison of land-surface parameterization schemes. *J. Hydrol.*, **212**, 128–135, doi:[10.1016/S0022-1694\(98\)00206-6](https://doi.org/10.1016/S0022-1694(98)00206-6).
- , and Coauthors, 1999: Key results and implications from phase 1(c) of the Project for Intercomparison of Land-Surface Parameterization Schemes. *Climate Dyn.*, **15**, 673–684, doi:[10.1007/s003820050309](https://doi.org/10.1007/s003820050309).
- Qu, W. Q., and Coauthors, 1998: Sensitivity of latent heat flux from PILPS land-surface schemes to perturbations of surface air temperature. *J. Atmos. Sci.*, **55**, 1909–1927, doi:[10.1175/1520-0469\(1998\)055<1909:SOLHFF>2.0.CO;2](https://doi.org/10.1175/1520-0469(1998)055<1909:SOLHFF>2.0.CO;2).
- Santanello, J. A., C. D. Peters-Lidard, S. V. Kumar, C. Alonge, and W. K. Tao, 2009: A modeling and observational framework for diagnosing local land–atmosphere coupling on diurnal time scales. *J. Hydrometeorol.*, **10**, 577–599, doi:[10.1175/2009JHM1066.1](https://doi.org/10.1175/2009JHM1066.1).
- Sen, O. L., W. J. Shuttleworth, and Z. L. Yang, 2000: Comparative evaluation of BATS2, BATS, and SiB2 with Amazon data. *J. Hydrometeorol.*, **1**, 135–153, doi:[10.1175/1525-7541\(2000\)001<0135:CEOBBA>2.0.CO;2](https://doi.org/10.1175/1525-7541(2000)001<0135:CEOBBA>2.0.CO;2).
- Stephens, G. L., and Coauthors, 2012: An update on Earth's energy balance in light of the latest global observations. *Nat. Geosci.*, **5**, 691–696, doi:[10.1038/ngeo1580](https://doi.org/10.1038/ngeo1580).
- Stöckli, R., and Coauthors., 2008: Use of FLUXNET in the Community Land Model development. *J. Geophys. Res.*, **113**, G01025, doi:[10.1029/2007JG000562](https://doi.org/10.1029/2007JG000562).
- Su, Z., P. de Rosnay, J. Wen, L. Wang, and Y. Zeng, 2013: Evaluation of ECMWF's soil moisture analyses using observations on the Tibetan Plateau. *J. Geophys. Res. Atmos.*, **118**, 5304–5318, doi:[10.1002/jgrd.50468](https://doi.org/10.1002/jgrd.50468).
- Szczypta, C., and Coauthors, 2011: Verification of the new ECMWF ERA-Interim reanalysis over France. *Hydrol. Earth Syst. Sci.*, **15**, 647–666, doi:[10.5194/hess-15-647-2011](https://doi.org/10.5194/hess-15-647-2011).
- Trémolet, Y., 2004: Diagnostics of linear and incremental approximations in 4D-Var. *Quart. J. Roy. Meteor. Soc.*, **130**, 2233–2251, doi:[10.1256/qj.03.33](https://doi.org/10.1256/qj.03.33).
- Twine, T. E., and Coauthors, 2000: Correcting eddy-covariance flux underestimates over a grassland. *Agric. For. Meteorol.*, **103**, 279–300, doi:[10.1016/S0168-1923\(00\)00123-4](https://doi.org/10.1016/S0168-1923(00)00123-4).
- Veerse, F., and J. N. Thepaut, 1998: Multiple-truncation incremental approach for four-dimensional variational data assimilation. *Quart. J. Roy. Meteor. Soc.*, **124**, 1889–1908, doi:[10.1002/qj.49712455006](https://doi.org/10.1002/qj.49712455006).
- Viterbo, P., and A. Beljaars, 1995: An improved land surface parameterization scheme in the ECMWF model and its validation. *J. Climate*, **8**, 2716–2748, doi:[10.1175/1520-0442\(1995\)008<2716:AILSPS>2.0.CO;2](https://doi.org/10.1175/1520-0442(1995)008<2716:AILSPS>2.0.CO;2).
- , —, J.-F. Mahfouf, and J. Teixeira, 1999: The representation of soil moisture freezing and its impact on the stable boundary layer. *Quart. J. Roy. Meteor. Soc.*, **125**, 2401–2426, doi:[10.1002/qj.49712555904](https://doi.org/10.1002/qj.49712555904).
- Wang, A. H., and X. B. Zeng, 2012: Evaluation of multi-reanalysis products with in situ observations over the Tibetan Plateau. *J. Geophys. Res.*, **117**, D05102, doi:[10.1029/2011JD016553](https://doi.org/10.1029/2011JD016553).
- Wang, K., 2010: Evidence for decadal variation in global terrestrial evapotranspiration between 1982 and 2002: 2. Results. *J. Geophys. Res.*, **115**, D20113, doi:[10.1029/2010JD013847](https://doi.org/10.1029/2010JD013847).
- , and R. E. Dickinson, 2012: A review of global terrestrial evapotranspiration: Observation, modeling, climatology, and climatic variability. *Rev. Geophys.*, **50**, RG2005, doi:[10.1029/2011RG000373](https://doi.org/10.1029/2011RG000373).
- , and —, 2013: Contribution of solar radiation to decadal temperature variability over land. *Proc. Natl. Acad. Sci. USA*, **110**, 14 877–14 882, doi:[10.1073/pnas.1311433110](https://doi.org/10.1073/pnas.1311433110).
- , —, M. Wild, and S. Liang, 2010: Evidence for decadal variation in global terrestrial evapotranspiration between 1982 and 2002: 1. Model development. *J. Geophys. Res.*, **115**, D20112, doi:[10.1029/2009JD013671](https://doi.org/10.1029/2009JD013671).
- Wilson, K., and Coauthors, 2002: Energy balance closure at FLUXNET sites. *Agric. For. Meteorol.*, **113**, 223–243, doi:[10.1016/S0168-1923\(02\)00109-0](https://doi.org/10.1016/S0168-1923(02)00109-0).
- Winter, J. M., and E. A. B. Eltahir, 2010: The sensitivity of latent heat flux to changes in the radiative forcing: A framework for comparing models and observations. *J. Climate*, **23**, 2345–2356, doi:[10.1175/2009JCLI1518.1](https://doi.org/10.1175/2009JCLI1518.1).
- Wood, E. F., and Coauthors, 1998: The Project for Intercomparison of Land-Surface Parameterization Schemes (PILPS) phase 2(c) Red–Arkansas River basin experiment: 1. Experiment description and summary intercomparisons. *Global Planet. Change*, **19**, 115–135, doi:[10.1016/S0921-8181\(98\)00044-7](https://doi.org/10.1016/S0921-8181(98)00044-7).
- Yao, Y., and Coauthors, 2014: Bayesian multimodel estimation of global terrestrial latent heat flux from eddy covariance, meteorological, and satellite observations. *J. Geophys. Res.*, **119**, 4521–4545, doi:[10.1002/2013JD020864](https://doi.org/10.1002/2013JD020864).